A minimum time control problem for aerobic degradation processes in biocell composting plants

Received: Added at production | Revised: Added at production | Accepted: Added at production

DOI: xxx/xxxx

ARTICLE TYPE

A minimum time control problem for aerobic degradation processes in biocell composting plants

G. Martalò*[1] | C. Bianchi[2] | B. Buonomo[3] | M. Chiappini[2] | V. Vespri[4]

[1]Department of Mathematical, Physical and Computer Sciences, University of Parma, Parma, Italy
[2]Istituto Nazionale di Geofisica e Vulcanologia (INGV), Rome, Italy
[3]Department of Mathematics and Applications, University of Naples Federico II, Naples, Italy
[4]Department of Mathematics and Computer Sciences *Ulisse Dini*, University of Florence, Florence, Italy

Correspondence
*G. Martalò, Department of Mathematical, Physical and Computer Sciences, University of Parma, Parco Area delle Scienze 53/A, 43124, Parma, Italy. Email: giorgio.martalo@unipr.it

Funding Information
This research was supported by the INdAM-INGV joint project SIES sponsored by MIUR (Progetto Premiale FOE2014).

Abstract

We introduce a mathematical model for the composting process in biocells. The model includes several phenomena, like the aerobic biodegradation of the soluble substrate by means of a bacterial population, the hydrolysis of insoluble substrate and the biomass decay. We investigate the best strategies to reduce substrate components in minimal time by controlling the effects of cell oxygen concentration on the degradation phenomenon. It is shown that singular controls are not optimal for this model and the optimal control time profiles are of bang or bang-bang type. The occurrence of switchings curve is discussed. In the case of a bang-bang control we prove that optimal control profiles have a unique switching time and the corresponding switching curve is determined.

KEYWORDS:
Composting; Waste management; Optimal control

1 | INTRODUCTION

Waste management is a current problem of great interest, especially for local authorities that have to decide the action strategies in their policy area[26]. A traditional approach, based on the stocking in a containment vessel, has already unclosed some criticisms, like the increasing requirement of new stocking sites and the formation and diffusion of leachate that can contaminate soil and aquifers[6,10]. For such reason, nowadays a landfill is conceived as a bioreactor, i.e. as a biological active environment where the natural and spontaneous phenomena of aerobic or anaerobic degradation play a crucial role and are strongly exploited for a satisfactory landfill performance[18,22].

In recent years, many mathematical models have been proposed in literature to describe both aerobic and anaerobic digestion phenomena (e.g.[2,4,11,14,28]) and applications to composting processes in static aerated piles[13] and windrows[24,25]. As pointed out in[11], many anaerobic models are often proposed with the main aim to combine accuracy and complexity. From this perspective, authors describe mathematically any phase of the degradation[14] and consider several effects, like leachate recirculation and pH adjustment[28]. Similarly, in composting descriptions[13,24,25], several distinctive features, like the distinction between slowly and rapidly degradable substrate and interactions with atmosphere, are taken into account to model accurately aerobic process in open systems. Although realistic, such models are not very treatable from a mathematical point of view and few qualitative results are available in literature[2,4].

In order to improve the performance of a landfill site it is possible to set a so-called optimal control problem and individuate the

best strategies to be adopted [1,3,15,16,23].

Different issues can be faced in this context and the subsequent strategies strictly depend both on the choice of the manipulated process and the goal to be reached. For example in [15,16] a mathematical description of an aerobic degradation process occurring in a composting biocell has been proposed. By controlling the oxygen injection, the best aeration strategies have been given to (i) maintain satisfactory levels of oxygen concentration in the cell, (ii) maximize the production of compost and (iii) minimize the cost of the aeration operation.

In [1], the authors propose a model for a continuously filled bioreactor controlled by its dilution rate with the goal of synthesizing optimal feeding strategies that maximize the biogas production over a time period. Other control strategies can be identified to reach a suitable target configuration in minimal time. For example, in [23], the leachate recirculation is the manipulated variable that is used for the reduction of solid waste below a given value.

In this paper, inspired by [24,25], we describe the digestion process in a composting cell, where an aerobic bacterial population degrades the organic fraction of solid waste. The organic matter is modeled as a two components substrate (soluble and insoluble). We also consider the main basic phenomena regulating the composting process [13] (i) the aerobic degradation: the bacterial population increases by consuming soluble substrate and oxygen; (ii) hydrolysis, i.e. the solubilization of the insoluble substrate; (iii) the biomass decay for which the bacteria death produces new insoluble substrate.

The main goal is the reduction of the substrate in minimal time by acting on the digestion process. The target is constituted by the set of configurations with both components of substrate below given thresholds. The control is obtained through a control function which models the effects of oxygen concentration on the degradation process. Such effects can be manipulated by means of an aspiration/injection system [20].

The paper is organized as follows: we present the mathematical model and some basic properties in Section 2 while in Section 3 the time optimal control problem is formulated and some preliminary results are discussed. The controllability set for any target and the optimal trajectories and control are determined respectively in Sections 4 and 5. Conclusions are given in Section 6.

2 | MODEL AND BASIC PROPERTIES

We propose a model that describes the action of an aerobic bacterial population degrading the organic fraction of the solid waste stocked in a biocell. The organic matter is represented as a two component substrate, where the soluble part is ready to be digested by bacteria while the insoluble one has to undergo a hydrolytic process. We consider also a biomass decay phenomenon. The model is governed by the following set of ordinary differential equations:

$$\begin{aligned} \frac{dS}{d\tau} &= -\mu\tilde{g}(S,\Omega)X + \tilde{c}_h I \\ \frac{dI}{d\tau} &= -\tilde{c}_h I + \tilde{b}X \\ \frac{dX}{d\tau} &= \mu\tilde{g}(S,\Omega)X - \tilde{b}X\,, \end{aligned} \tag{1}$$

where τ is the time variable, $S(\tau)$, $I(\tau)$ and $X(\tau)$ denote the soluble substrate, the insoluble substrate and the bacterial biomass at time τ respectively; $\Omega(\tau)$ is the oxygen concentration in the cell atmosphere at time τ; $\mu\tilde{g}(S,\Omega)X$ represents the growth rate of biomass [25]. The positive constants μ, $\tilde{b}$ and $\tilde{c}_h$ represent the maximal growth rate, the biomass decay and hydrolysis coefficients, respectively.

We use the total mass conservation

$$\mathcal{M}(\tau) = S(\tau) + I(\tau) + X(\tau) = S(0) + I(0) + X(0) = \mathcal{M}(0) =: m \tag{2}$$

to introduce the following scaling

$$t = \mu\tau\,,\ s = \frac{S}{m}\,,\ i = \frac{I}{m}\,,\ x = \frac{X}{m}\,,\ \omega = \frac{\Omega}{\Omega_0}\,, \tag{3}$$

where $0 \le s, i, x \le 1$, $\omega \ge 0$ and Ω_0 is a given oxygen concentration value corresponding to the fastest substrate degradation [7,26]. We consider also a restriction on the oxygen level in the cell atmosphere, $\omega \in [0, \omega_{\max}]$ [10].

The nondimensional system of equations reads

$$\begin{aligned} \frac{ds}{dt} &= -g(s,\omega)(1-s-i) + c_h i \\ \frac{di}{dt} &= -c_h i + b(1-s-i)\,, \end{aligned} \tag{4}$$

where the conservation law (2) is used to replace x by $1-s-i$.
As concerns the biomass growth function, we introduce the following factorization [9,13,24,25]

$$g(s,\omega) = g_1(s)\, g_2(\omega)\,, \tag{5}$$

where $g_1(s)$ and $g_2(\omega)$ describe the effects of substrate and oxygen concentrations on the degradation process, respectively. We require that

H1 - $g_1(0) = 0$ and $g_1(s) > 0$ for any $s \in (0,1]$,

H2 - $g_1 \in C^1([0,1])$, $g_1'(s) > 0$ for any $s \in [0,1]$,

H3 - $g_2(0) = 0$ and $g_2(\omega) > 0$ for any $\omega \in \left(0, \omega_{\max}\right]$,

H4 - $g_2 \in C^1\left(\left[0, \omega_{\max}\right]\right)$, $g_2'(\omega) > 0$ for any $\omega \in \left[0, \omega_{\max}\right]$.

These hypothesis are satisfied by Monod functions, typically used in models for bacterial culture growth, given by [17]:

$$g_1(s) = \frac{s}{c_s + s}\,, \qquad g_2(\omega) = \frac{\omega}{c_\omega + \omega}\,, \tag{6}$$

where c_s and c_ω are the half-saturation constants.
Under the hypothesis **H3** and **H4**, we introduce a control function

$$u(t) \in \mathcal{U} := \left\{ \nu \,:\, [0,\infty) \longrightarrow \left[0, u_{\max}\right] \,,\ \nu \text{ Lebesgue measurable} \right\} \tag{7}$$

modeling the effects of the oxygen concentration on the degradation rate.
Model (4) can be written as

$$\begin{aligned} \frac{ds}{dt} &= -u(t)\, g_1(s)(1-s-i) + c_h i \\ \frac{di}{dt} &= -c_h i + b(1-s-i)\,. \end{aligned} \tag{8}$$

Without any loss of generality we also set $u_{\max} = 1$.
It can be easily checked that hypothesis **H1** ensures that the set

$$\mathcal{F} = \{(s,i) \in [0,1] \times [0,1] \ \text{ such that } s + i \le 1\} \tag{9}$$

is positively invariant. Therefore, the solutions of (8) corresponding to nonnegative initial values, $s(0) = s_0 \ge 0$, $i(0) = i_0 \ge 0$, remain nonnegative for any $t > 0$.

2.1 | Basic properties for a well aerated cell

In view of the optimal synthesis that will be presented in next sections, we briefly discuss some basic properties of model (8) when a suitable aeration strategy guarantees the same constant level of oxygen, θ, at any time, i.e. $u(t) = \theta \in [0,1]$ for any $t > 0$.
It is easy to verify that the point $E_0 = (1,0) \in \mathcal{F}$ is a steady solution of

$$\begin{aligned} \frac{ds}{dt} &= -\theta g_1(s)(1-s-i) + c_h i \\ \frac{di}{dt} &= -c_h i + b(1-s-i)\,, \end{aligned} \tag{10}$$

for any value of the parameter $\theta \in [0,1]$. Such configuration corresponds to the absence of the bacterial population and the insoluble substrate: the total mass m is given by the soluble substrate.
If $\theta \neq 0$, the system (10) may admit another equilibrium state $E_1^\theta = \left(\tilde{s}, \tilde{i}\right)$ where $\tilde{s}$ is solution of $\theta g_1(s) - b = 0$ in $[0,1]$ and $\tilde{i} = b(1-\tilde{s}) \,/\, \left(c_h + b\right)$. We observe that the existence of E_1^θ strictly depends on the specific response functional considered and, when it exists, $E_1^\theta \in \mathcal{F}$, since

$$0 \le \tilde{i} < \tilde{s} + \tilde{i} \le 1\,. \tag{11}$$

Physically, at equilibrium E_1^θ, the bacterial population can survive because of the aeration strategy that guarantees a sufficient level of oxygen for its growth and balances the death term.

The linear stability of equilibria may be investigated in a standard way by using linearization method, i.e. by computing the eigenvalues of the Jacobian matrix, say $J(E)$, associated to (10) evaluated at the equilibrium. More precisely, if both the eigenvalues of $J(E)$ have negative real part then E is locally stable. If at least one eigenvalue of $J(E)$ has positive real part then E is locally unstable.

It is easy to check that E_0 is linearly stable if $u < b/g_1(1)$ while E_1^θ is linearly stable when it exists. It follows that it can exist a bifurcation value of θ, say $\tilde{\theta}$ in correspondence of which the equilibrium E_1^θ emerges and E_0 changes its stability; moreover the equilibrium E_1^θ belongs to

$$C_2 = \left\{ (s,i) \in \mathcal{F} \text{ such that } g_1^{-1}(b) \leq s \leq 1 \,,\, i = \frac{b(1-s)}{b+c_h} \right\} , \tag{12}$$

for any $\tilde{\theta} \leq \theta \leq 1$.

We can observe that this result is obtained under the hypothesis **H2**; a little more complicated scenario arises when such assumption is relaxed since the equation $ug_1(s) - b = 0$ could not have a unique solution.

As last remark, we observe that the local stability here implies the global stability since we can exclude the occurrence of periodic solutions as a simple direct application of the Dulac criterion [19].

The bifurcation diagram when the biomass growth function is of Monod type (6) is depicted in Figure 1. The parameters values used to obtain Figure 1 and all the other plots in this paper are the purely theoretical baseline values:

$$c_s = 0.417 \,,\; c_h = 0.245 \,,\; b = 0.19 \,. \tag{13}$$

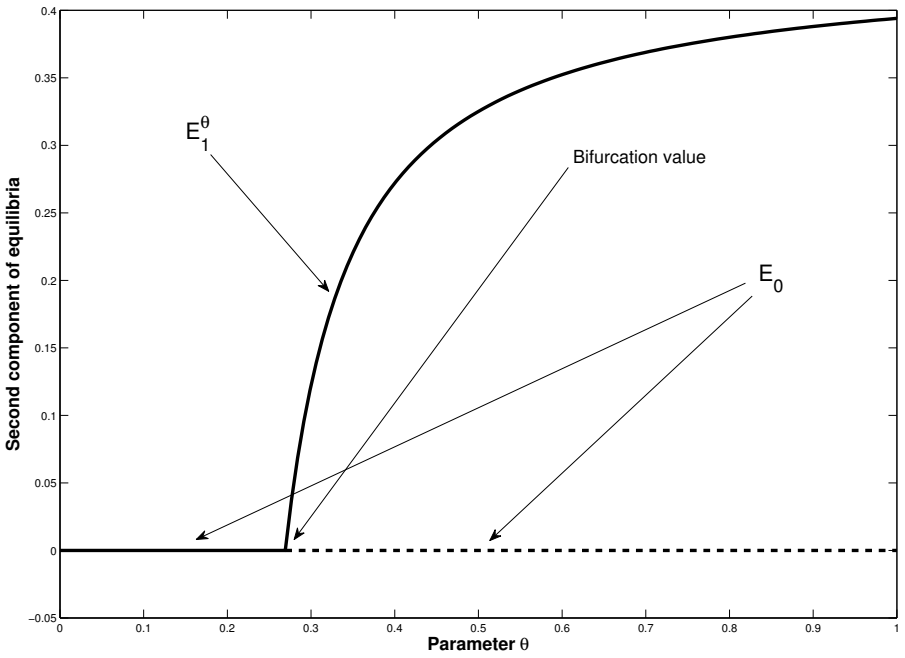

FIGURE 1 Bifurcation diagram in presence of Monod response functions (6): second component of equilibria versus bifurcation parameter θ. Parameter values are given in (13). The bifurcation value for θ is $\tilde{\theta} = 0.26923$. Continuous line denotes stability, dashed line indicates instability.

3 | TIME OPTIMAL CONTROL PROBLEM

In this section we formulate a minimum time problem whose purpose is the reduction of both substrate components under a given threshold. Physically this corresponds to individuate the best strategy to consume the organic fraction of solid waste in the fastest way in order to increase the capacity of a composting plant.
Mathematically, we consider a state $\mathbf{z}^* = (s^*, i^*)$, whose components indicate the given thresholds for soluble and insoluble substrate, respectively, and we denote by $\mathcal{T} = [0, s^*] \times [0, i^*] \subset \mathcal{F}$ the target set.
Our aim is to determine the optimal control function $u(t)$ in the admissible control function set $\mathcal{U}$ given in (7) that drives the state vector $(s(t), i(t))$ from an initial configuration $\mathbf{z}_0 = (s_0, i_0) \in \mathcal{F} \setminus \mathcal{T}$ to "touch" the target $\mathcal{T}$ in $\partial\mathcal{T}$ in the minimal time.
More precisely, we indicate by $\mathbf{z}_u = (s_u, i_u)$ the unique solution of (8) associated to a given control function $u(t)$ and initial condition $\mathbf{z}_0$. Our aim is to find

$$\inf_{u(t)\in\mathcal{U}} t_u \text{ such that } s_u(t_u) \le s^* \text{ and } i_u(t_u) \le i^* . \tag{14}$$

The existence of the time optimal control is guaranteed, since the model (8) depends linearly on the control variable u and the set of admissible controls $\mathcal{U}$ given in (7) is convex and compact (see Therorem 4.3 in [12]).
The optimal control problem can be formulated in terms of a suitable Hamiltonian function, by using the Pontryagin's maximum principle (PMP)[21]. Let $u(t)$ be an optimal control function steering the initial state $\mathbf{z}_0 \in \mathcal{F} \setminus \mathcal{T}$ to the target $\mathcal{T}$ in minimal time; let $\mathbf{z}(\cdot) = (s(\cdot), i(\cdot)) : [0, t_f] \longrightarrow \mathbb{R}^2$ the associated trajectory defined on the time interval $[0, t_f]$, where $t_f > 0$ and $\mathbf{z}(t_f) \in \partial\mathcal{T}$.
Then, according to PMP, there exists $\lambda_0 \in \mathbb{R}_-$ and an absolutely continuous map $\Lambda(\cdot) = (\lambda_s(\cdot), \lambda_i(\cdot)) : [0, t_f] \longrightarrow \mathbb{R}^2$ such that $(\lambda_0, \lambda_s(\cdot), \lambda_i(\cdot)) \neq 0$ and solves the adjoint system

$$\begin{aligned} \dot\lambda_s &= -\frac{\partial\mathcal{H}}{\partial s} = \lambda_s u\left[g_1'(s)(1-s-i) - g_1(s)\right] + \lambda_i b \\ \dot\lambda_i &= -\frac{\partial\mathcal{H}}{\partial i} = -\lambda_s\left[u g_1(s) + c_h\right] + \lambda_i\left(c_h + b\right) , \end{aligned} \tag{15}$$

where the upper dots denote the derivative with respect to variable t and

$$\begin{aligned} \mathcal{H} \;:\; & \mathcal{F} \times \mathbb{R}^2 \times \mathbb{R}_- \times [0,1] \longrightarrow \mathbb{R} \\ & (s, i, \lambda_s, \lambda_i, \lambda_0, u) \longrightarrow \lambda_0 - u\lambda_s g_1(s)(1-s-i) + \left(\lambda_s - \lambda_i\right) c_h i + \lambda_i b (1-s-i) \end{aligned} \tag{16}$$

is the Hamiltonian function and the control $u(t)$ is such that

$$u(t) \in \operatorname{argmax}_{\alpha\in[0,1]} \mathcal{H}\left(s(t), i(t), \lambda_s(t), \lambda_i(t), \lambda_0, \alpha\right) , \tag{17}$$

a.e. $t \in [0, t_f]$. A triplet $(\mathbf{z}, \Lambda, u)$ satisfying (8), (15) and (17) is called *extremal trajectory*. When $\lambda_0 = 0$ we say that an extremal trajectory is *abnormal* whereas if $\lambda_0 \neq 0$ it is *normal*. As t_f is free, $\mathcal{H}$ is equal to 0 along any extremal trajectory[5].
Finally, the optimal control $\tilde u(t)$ satisfies the control law

$$\tilde u(t) = \begin{cases} 0 & \text{for } \phi(t) < 0 \\ u \in (0,1) & \text{for } \phi(t) = 0 \\ 1 & \text{for } \phi(t) > 0 , \end{cases} \tag{18}$$

where the function

$$\phi = \frac{\partial\mathcal{H}}{\partial u} = -\lambda_s g_1(s)(1-s-i) , \tag{19}$$

is called *switching function*[8,27].

3.1 | Singular trajectories and predicting switching

Let us give some useful definitions.
A time $t_r \in (0, t_f)$ is called *regular* if $\phi(t_r) \neq 0$. A *switiching time* $t_s \in (0, t_f)$ is a non-regular time (i.e. $\phi(t_s) = 0$) at which the switching function changes sign[5].
An extremal trajectory has a *singular arc* (the trajectory is said *singular*) if there exists a time interval $[t_1, t_2] \subset [0, t_f]$ where $\phi(t) = 0$ for any $t \in [t_1, t_2]$. The corresponding control $u(t)$, for $t_1 \le t \le t_2$, is called *singular control*.
We rewrite the dynamical system (8) as

$$\dot{\mathbf{z}} = \xi(\mathbf{z}) + u\eta(\mathbf{z}) \tag{20}$$

and define the *collinearity curve* as the the set of points of $\mathcal{F}$ where ξ and η are collinear, i.e.

$$\Delta_0 := \left\{ \mathbf{z} = (s,i) \in \mathcal{F} \text{ such that } f_0(\mathbf{z}) = \det\left[\xi(\mathbf{z}), \eta(\mathbf{z})\right] = 0 \right\} . \tag{21}$$

The *singular locus* is defined as the subset of $\mathcal{F}$ of codimension 1 to which a singular trajectory belongs and is individuated as

$$\Delta_1 := \left\{ \mathbf{z} = (s,i) \in \mathcal{F} \text{ such that } f_1(\mathbf{z}) = \det\left[\eta(\mathbf{z}), < \xi, \eta > (\mathbf{z})\right] = 0 \right\} , \tag{22}$$

where $< \cdot, \cdot >$ denotes the Lie bracket.
The vector functions ξ and η are given by

$$\xi = \begin{pmatrix} c_h i \\ -c_h i + b(1-s-i) \end{pmatrix} , \qquad \eta = \begin{pmatrix} -g_1(s)(1-s-i) \\ 0 \end{pmatrix} ; \tag{23}$$

therefore we have

$$f_0(s,i) = g_1(s)(1-s-i)\left[-c_h i + b(1-s-i)\right] , \qquad f_1(s,i) = b g_1^2(s)(1-s-i)^2 , \tag{24}$$

defining respectively the collinearity curve Δ_0 and the singular locus Δ_1 as

$$\Delta_0 = \left\{ (s,i) \in \mathcal{F} \text{ such that } f_0(s,i) = 0 \right\} , \qquad \Delta_1 = \left\{ (s,i) \in \mathcal{F} \text{ such that } f_1(s,i) = 0 \right\} \tag{25}$$

or, equivalently,

$$\begin{aligned} \Delta_0 &= \{(s,i) \in \mathcal{F} \ : \ s = 0\} \cup \{(s,i) \in \mathcal{F} \ : \ s + i = 1\} \cup \left\{ (s,i) \in \mathcal{F} \ : \ i = \frac{b(1-s)}{c_h + b} \right\} , \\ \Delta_1 &= \{(s,i) \in \mathcal{F} \ : \ s = 0\} \cup \{(s,i) \in \mathcal{F} \ : \ s + i = 1\} . \end{aligned} \tag{26}$$

We can notice that $\Delta_1 \cap \mathrm{Int}(\mathcal{F}) = \emptyset$, where $\mathrm{Int}(\mathcal{F})$ denotes the interior of the set $\mathcal{F}$. Therefore, we can exclude the occurrence of singular trajectory and the optimal control cannot exhibit a singular arc. This means that the optimal control function is constant (*bang control*) or piecewise constant (*bang-bang control*), where the control passes instantaneously from 0 to 1 or viceversa at any switching time.

Proposition 1. Let $(\mathbf{z}, \Lambda, u)$ be a normal extremal trajectory. Then

(i) there exists a function $h : \mathbb{R} \times \left(\mathcal{F} \setminus \Delta_0\right) \longrightarrow \mathbb{R}$, $(u,s,i) \longrightarrow h(u,s,i)$ such that

$$\dot{\phi}(t) = h(u(t), s(t), i(t))\,\phi(t) - \frac{f_1(s(t), i(t))}{f_0(s(t), i(t))} , \tag{27}$$

a.e. $t \in [0, t_f]$;

(ii) let us introduce

$$\mathcal{S}_{\pm} = \left\{ (s,i) \in \mathcal{F} \text{ such that } \frac{f_1(s(t), i(t))}{f_0(s(t), i(t))} \gtrless 0 \right\} . \tag{28}$$

If the extremal trajectory is optimal then at any switching time t_s such that $\left(s\left(t_s\right), i\left(t_s\right)\right) \in \mathcal{S}_+$ (respectively $\left(s\left(t_s\right), i\left(t_s\right)\right) \in \mathcal{S}_-$) the control passes from 1 to 0 (respectively from 0 to 1).

Proof. *(i)* From (19) we can write the adjoint variable λ_s in terms of the switching function ϕ as

$$\lambda_s = -\frac{\phi}{g_1(s)(1-s-i)} ; \tag{29}$$

since $(\mathbf{z}, \Lambda, u)$ is a normal extremal trajectory, $\mathcal{H} = 0$ along the trajectory and we can set $\lambda_0 = -1$. It follows that

$$\lambda_i = \frac{1 - u\phi - \lambda_s c_h i}{-c_h i + b(1-s-i)} = \frac{1 - u\phi + \dfrac{\phi c_h i}{g_1(s)(1-s-i)}}{-c_h i + b(1-s-i)} , \tag{30}$$

where formula (29) is used in the last equality. By substitution in

$$\dot{\phi}(t) = \left[\left(\lambda_s(t) - \lambda_i(t)\right) b g_1(s(t)) - \lambda_s(t)\, c_h g_1'(s(t))\, i(t)\right](1 - s(t) - i(t)) , \tag{31}$$

we obtain (27).
(ii) Let us suppose that there exists a switching time t_s in correspondence of which the control passes from 0 to 1 in a state of $\mathcal{S}_+$. Since t_s is a switching time it follows that $\phi\left(t_s\right) = 0$. Moreover there exists $\varepsilon > 0$ such that $u = 0$ in $(t_s - \varepsilon, t_s)$; it follows

that $\dot{\phi}\left(t_s\right) \geq 0$.
From (27) we have

$$\frac{f_1\left(s\left(t_s\right), i\left(t_s\right)\right)}{f_0\left(s\left(t_s\right), i\left(t_s\right)\right)} = h\left(u\left(t_s\right), s\left(t_s\right), i\left(t_s\right)\right)\phi\left(t_s\right) - \dot{\phi}\left(t_s\right) \leq 0\,, \tag{32}$$

in contradiction with the hypothesis that the switching occurs in $\mathcal{S}_+$, i.e. $\dfrac{f_1\left(s\left(t_s\right), i\left(t_s\right)\right)}{f_0\left(s\left(t_s\right), i\left(t_s\right)\right)} > 0$. □

4 | CONTROLLABILITY RESULTS

We are now interested in finding the *controllability set* for any admissible target $\mathcal{T} = [0, s^*] \times [0, i^*] \subset \mathcal{F}$, i.e. the set of points $\mathbf{z}_0 = (s_0, i_0) \in \mathcal{F} \setminus \mathcal{T}$ for which there exists an admissible control $u \in \mathcal{U}$ such that the trajectory starting from $\mathbf{z}_0$ with control u reaches a configuration in $\mathcal{T}$ in finite time.
The characterization of the controllability set will strongly depend on the position of the vertex $\mathbf{z}^*$ of $\mathcal{T}$ in $\mathcal{F}$. For such reason we consider a possible partition of the invariant set $\mathcal{F}$ and discuss different cases.
Let us introduce the following curves (see Figure 2(a))

$$\begin{aligned}
\mathcal{J}_0 &= \{(s,i) \in \partial\mathcal{F} \text{ such that } i = 0\}\,,\\
\mathcal{J}_1 &= \left\{(s,i) \in \partial\mathcal{F} \text{ such that } g_1^{-1}(b) \leq s \leq 1\,,\ i = 1-s\right\}\,,\\
\mathcal{J}_2 &= \left\{(s,i) \in \partial\mathcal{F} \text{ such that } 0 \leq s \leq g_1^{-1}(b)\,,\ i = 1-s\right\} \cup \{(s,i) \in \partial\mathcal{F} \text{ such that } s = 0\}\,,\\
\mathcal{C}_0 &= \left\{(s,i) \in \mathcal{F} \text{ such that } s = g_1^{-1}(b)\,,\ \frac{b\left(1-g_1^{-1}(b)\right)}{b+c_h} \leq i \leq 1\right\}\,,\\
\mathcal{C}_1 &= \left\{(s,i) \in \mathcal{F} \text{ such that } 0 \leq s \leq g_1^{-1}(b)\,,\ i = \frac{g_1(s)(1-s)}{g_1(s)+c_h}\right\}\,,
\end{aligned} \tag{33}$$

and $\mathcal{C}_2$ given in (12). These curves give the partition

$$\mathcal{F} = \mathcal{F}_0 \cup \mathcal{F}_1 \cup \mathcal{F}_2\,, \tag{34}$$

where

- $\mathcal{F}_0$ is bounded by $\mathcal{C}_0$, $\mathcal{C}_1$ and $\mathcal{J}_2$;
- $\mathcal{F}_1$ is bounded by $\mathcal{J}_0$, $\mathcal{C}_1$ and $\mathcal{C}_2$;
- $\mathcal{F}_2$ is bounded by $\mathcal{C}_0$, $\mathcal{J}_1$ and $\mathcal{C}_2$.

The partition of $\mathcal{F}$ is depicted in Figure 2(b) in the case of Monod response functions (6).
We denote by $\Gamma_u^{\mathbf{z}}$ the backward solution of (8) with control $u \in \mathcal{U}$ from 0 to $t_u^{\mathbf{z}}$, where $t_u^{\mathbf{z}}$ is the first time in correspondence of which the backward solution intersects the boundary of $\mathcal{F}$.

4.1 | Case I : $\mathbf{z}^* \in \mathcal{F}_0$

Let us consider the backward solutions of (8) with constant control $u = 1$ starting from $\mathbf{z}^*$ (denoted by $\Gamma_1^{\mathbf{z}^*}$) and from $\mathbf{z}^{\#}$ (denoted by $\Gamma_1^{\mathbf{z}^{\#}}$), where $\mathbf{z}^{\#}$ is the intersection between the boundary of $\mathcal{T}$ and C_1. $\Gamma_1^{\mathbf{z}^{\#}}$ intersects the boundary $\partial\mathcal{F}$ in $\mathcal{J}_0$ or $\mathcal{J}_2$ according to the position of $\mathbf{z}^{\#}$ on the curve C_1.
We consider two subsets $\mathcal{S}_1$ and $\mathcal{S}_2$ in $\mathcal{F}$; more precisely

- if $\Gamma_1^{\mathbf{z}^*}$ does not intersect the target set $\mathcal{T}$, $\mathcal{S}_1$ is the subset of $\mathcal{F}$ bounded by $\Gamma_1^{\mathbf{z}^*}$, the boundary of $\mathcal{F}$ and the line $i = i^*$; otherwise, such set $\mathcal{S}_1$ is a subset of $\mathcal{T}$ and the controllability result follows trivially;
- the set $\Gamma_1^{\mathbf{z}^{\#}} \cup \left\{(s,i) \in \mathcal{F} \ :\ s = s^*\,,\ 0 \leq i \leq i^{\#}\right\}$ partitions $\mathcal{F}$ in two disjoint components; $\mathcal{S}_2$ is the component that does not contain the intersection point $\mathcal{C}_0 \cap \mathcal{C}_1 \cap \mathcal{C}_2$.

Different scenarios are depicted in Figure 3 in the case of Monod response functions.

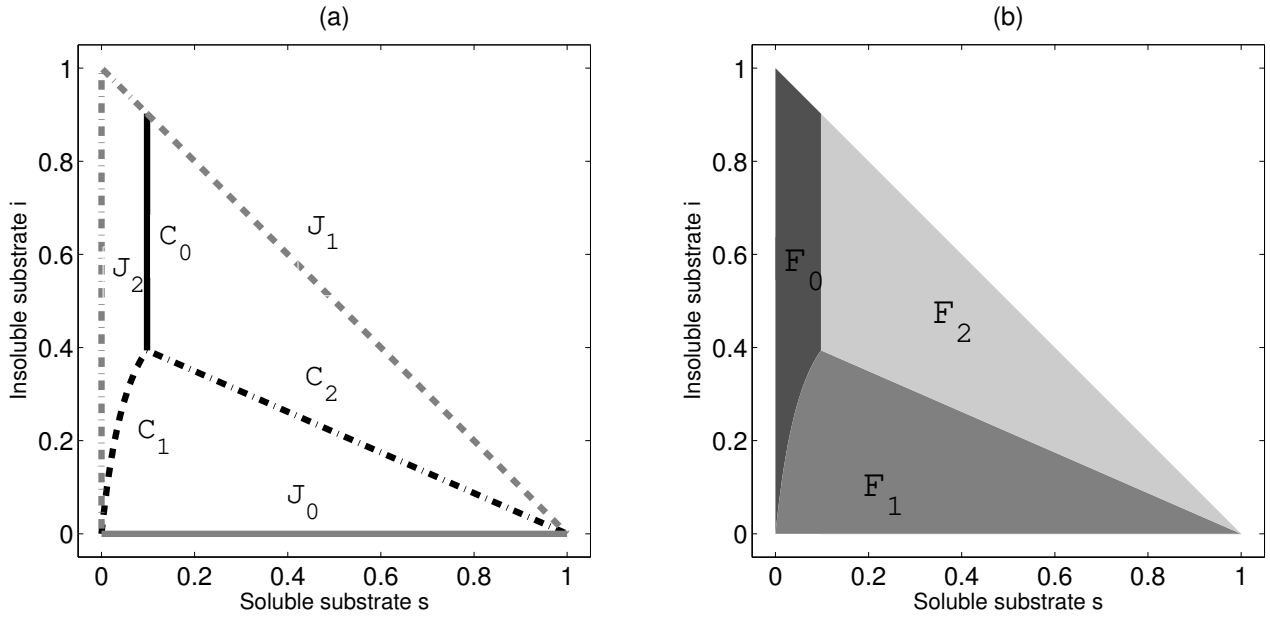

FIGURE 2 (a) The curves $\mathcal{C}_i$ and $\mathcal{J}_i$, $i = 0, 1, 2$ and (b) the partition of $\mathcal{F}$ in the case of a Monod response function (6). The parameters values are given in (13).

Proposition 2. (i) If $\mathbf{z}^* \in \mathcal{F}_0$ then the target $\mathcal{T}$ is reachable from any point $\mathbf{z}_0 = (s_0, i_0) \in \mathcal{S}_1 \cup \mathcal{S}_2$. (ii) If $\Gamma_1^{\mathbf{z}^\#} \cap \mathcal{J}_2 \neq \emptyset$ (see panels (b) and (d) in Figure 3) then the controllability set is given by $\mathcal{F}$.

Proof. Let us consider a state $\mathbf{z}_0 = (s_0, i_0) \in \mathcal{S}_1$ and the associated solution with constant control $u = 1$. This trajectory is asymptotically attracted by the stable equilibrium E_1^1 (which is given by $\mathcal{C}_0 \cap \mathcal{C}_1 \cap \mathcal{C}_2$) and cannot intersect $\Gamma_1^{\mathbf{z}^*}$, since $\Gamma_1^{\mathbf{z}^*}$ can be seen as the trajectory of the forward solution starting from $\tilde{\mathbf{z}} = \Gamma_1^{\mathbf{z}^*} \cap \mathcal{J}_2$. It follows that the solution starting from $\mathbf{z}_0$ can reach E_1^1 asymptotically passing through the set $\mathcal{T}$; more precisely it crosses $\partial\mathcal{T}$ in the upper horizontal edge.
Analogously we can prove that the target is reachable from $\mathbf{z}_0 = (s_0, i_0) \in \mathcal{S}_2$ assuming constant control $u = 1$. This proves point (i).
As for (ii), assume that $\Gamma_1^{\mathbf{z}^\#} \cap \mathcal{J}_2 \neq \emptyset$ (panels (b) and (d) in Figure 3) and consider an initial configuration $\mathbf{z}_0 = (s_0, i_0) \in \mathcal{F} \setminus \left(\mathcal{T} \cup \mathcal{S}_1 \cup \mathcal{S}_2\right)$. The solution starting from $\mathbf{z}_0$ with constant control $u = 0$ is asymptotically attracted by $E_0 = (1, 0)$; this means that it intersects the subset $\mathbf{S}_2$ in a finite time. Therefore the target $\mathcal{T}$ can be reached by considering a piecewise constant control: the control is $u = 0$ until the corresponding solution crosses $\mathcal{S}_2$; then it switches from 0 to 1 until reaching $\mathcal{T}$. □

4.2 | Case II : $\mathbf{z}^* \in \mathcal{F}_1$

Let us consider the backward solutions $\Gamma_1^{\mathbf{z}^*}$ starting from $\mathbf{z}^*$ with constant control $u = 1$. We can observe that $\Gamma_1^{\mathbf{z}^*} \cup \{(s, i) \in \mathcal{F} \ : \ s = s^*, \ 0 \leq i \leq i^*\}$ partitions $\mathcal{F}$ in two disjoint components; $\mathcal{S}$ is the component that does not contain the intersection $\mathcal{C}_0 \cap \mathcal{C}_1 \cap \mathcal{C}_2$.
We can observe that $\Gamma_1^{\mathbf{z}^*}$ intersects the boundary $\partial\mathcal{F}$ in $\mathcal{J}_0$ or $\mathcal{J}_2$ according to the position of $\mathbf{z}^*$ in $\mathcal{F}_1$.
Different scenarios are depicted in Figure 4 in the case of Monod response functions.

Proposition 3. (i) If $\mathbf{z}^* \in \mathcal{F}_1$ then the target $\mathcal{T}$ is reachable from any point $\mathbf{z}_0 = (s_0, i_0) \in \mathcal{S}$. (ii) If $\Gamma_1^{\mathbf{z}^*} \cap \mathcal{J}_2 \neq \emptyset$ (see panel (b) in Figure 4) then the controllability set is given by $\mathcal{F}$.

Proof. The results can be proved as in Proposition 2. □

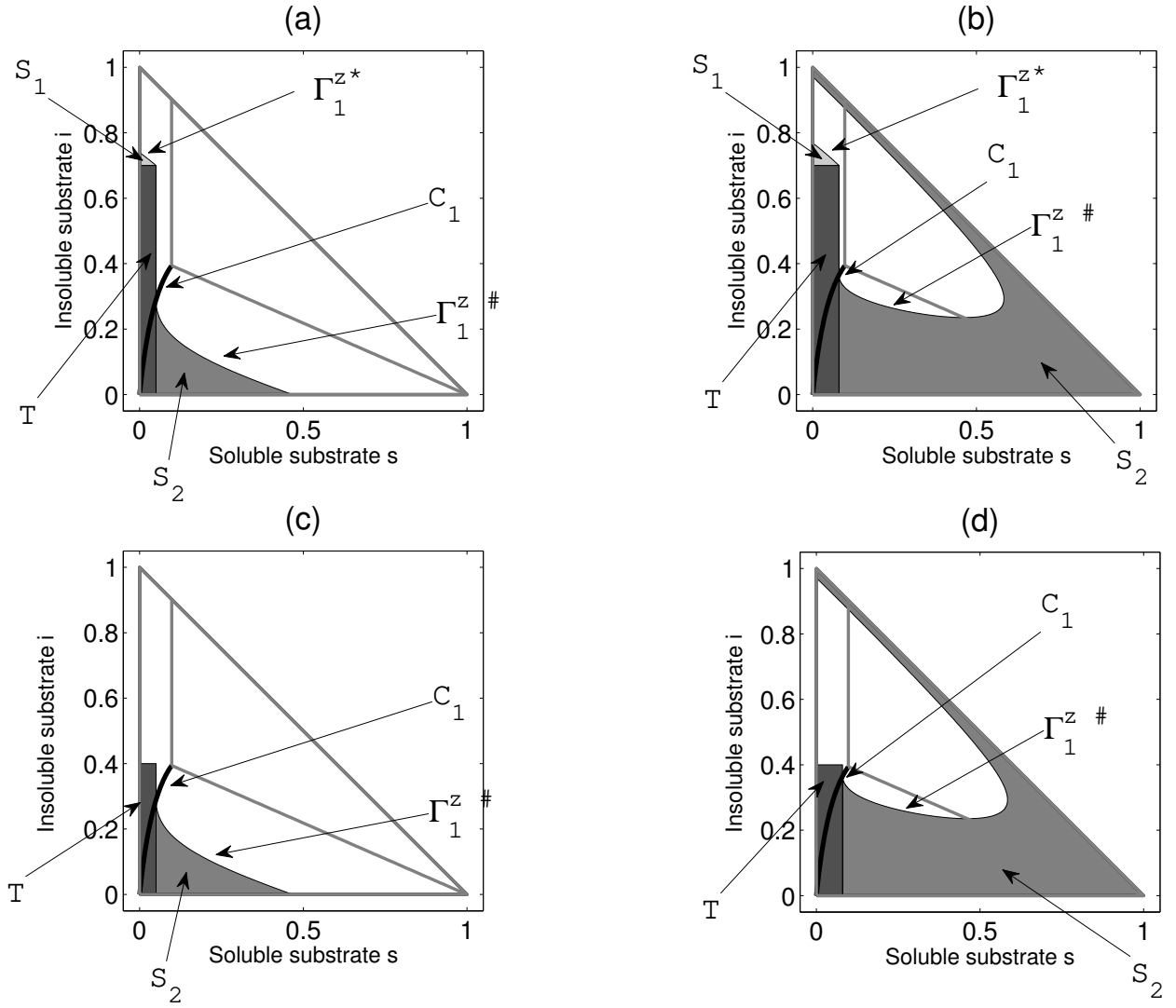

FIGURE 3 Controllability sets $\mathcal{S}_1$ and $\mathcal{S}_2$ when $\mathbf{z}^* \in \mathcal{F}_0$ in the case of Monod response functions (6). The (nondimensional) parameter values are given in (13). In panels (c) and (d) the set $\mathcal{S}_1$ is such that $\mathcal{S}_1 \subset \mathcal{T}$ and not indicated in the plot. In panels (a) and (c) $\Gamma_1^{\mathbf{z}^\#}$ intersects $\mathcal{J}_0$. In panels (b) and (d) $\Gamma_1^{\mathbf{z}^\#}$ intersects $\mathcal{J}_2$.

4.3 | Case III : $\mathbf{z}^* \in \mathcal{F}_2$

Proposition 4. If $\mathbf{z}^* \in \mathcal{F}_2$ then the controllability set for target $\mathcal{T}$ is $\mathcal{F}$.

Proof. We can observe that when $\mathbf{z}^* \in \mathcal{F}_2$ it follows that $\mathcal{T} \cap C_2 \neq \emptyset$; this means (see Subsection 2.1) that there exists a parameter $u_0 \in [0, 1]$ such that the equilibrium $E_1^{u_0} \in \mathcal{T} \cap C_2$ and is asymptotically stable (see Figure 5(a)).
For any $\mathbf{z}_0 \in \mathcal{F} \setminus \mathcal{T}$, the forward solution starting from it with constant control $u = u_0$ is asymptotically attracted by $E_1^{u_0}$ and, as consequence, the target $\mathcal{T}$ is reachable in a finite time. □

As done in the previous subsections, also in this case we can individuate some suitable subsets $\mathcal{S}_1$ and $\mathcal{S}_2$. We can observe that $\Gamma_1^{\mathbf{z}^*} \cup \{(s, i) \in \mathcal{F} \ : \ s = s^* \, , \, 0 \leq i \leq i^*\}$ partitions $\mathcal{F}$ in two disjoint components; $\mathcal{S}_2$ is the component that does not contain the intersection $C_0 \cap C_1 \cap C_2$ while $\mathcal{S}_1 = \mathcal{F} \setminus \left(\mathcal{T} \cup \mathcal{S}_2\right)$ (see Figure 5(b) for Monod response functionals).
Since $\Gamma_0^{\mathbf{z}^*}$, corresponding to $u = 0$, partitions $\mathcal{S}_1$, we denote by $\mathcal{S}_1^{(1)}$ the subset bounded by $\Gamma_0^{\mathbf{z}^*}$ and the horizontal edge of $\mathcal{T}$ and by $\mathcal{S}_1^{(2)}$ the remaining part.

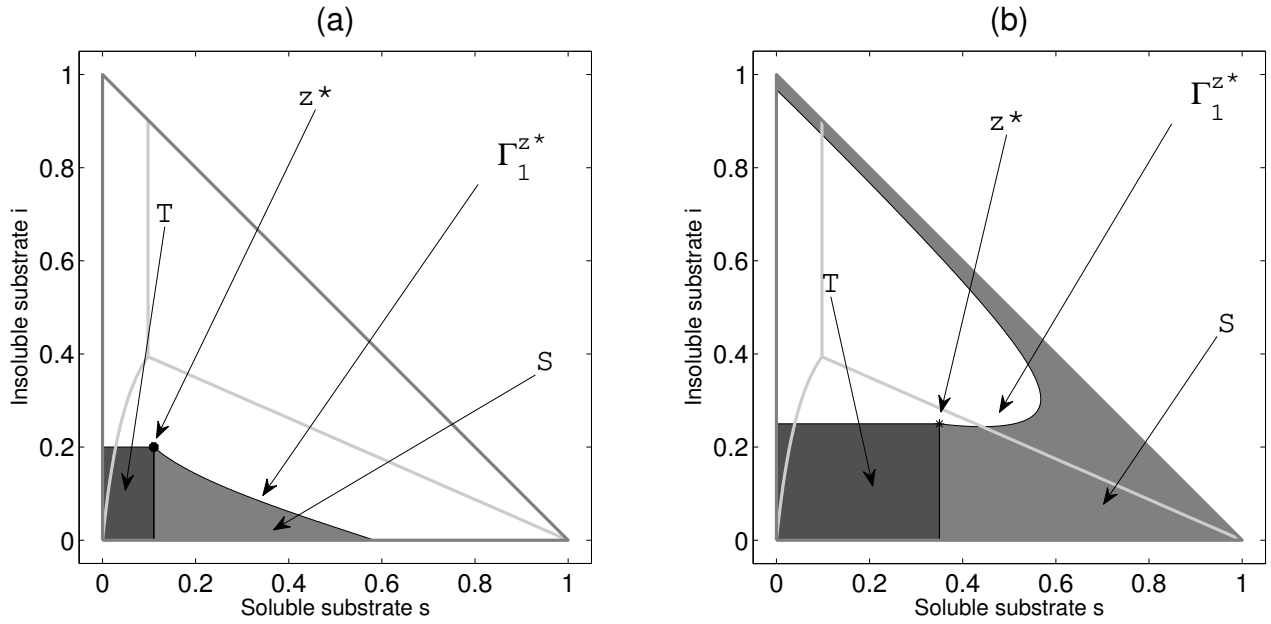

FIGURE 4 Controllability set $\mathcal{S}$ when $\mathbf{z}^* \in \mathcal{F}_1$ for Monod response functions (6). The nondimensional parameters values are given in (13). In panel (a) $\Gamma_1^{\mathbf{z}^\#}$ intersects $\mathcal{J}_0$ while in panel (b) it intersects $\mathcal{J}_2$.

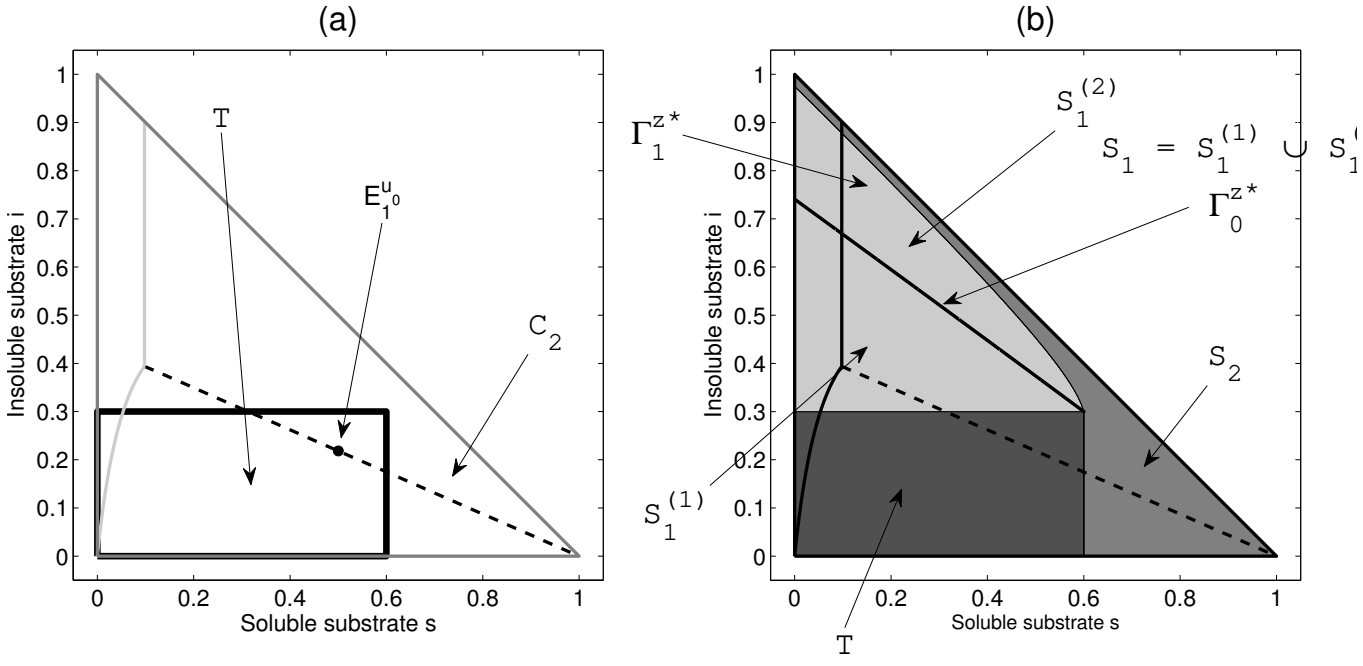

FIGURE 5 Controllability results and subsets $\mathcal{S}_1^{(1)}$, $\mathcal{S}_1^{(2)}$ and $\mathcal{S}_2$ when $\mathbf{z}^* \in \mathcal{F}_2$ in the case of Monod response functions (6). The parameters values are given in (13).

5 | OPTIMAL CONTROLS

In this section we look for optimal control in the admissible control function set (7) that drives the state vector of model (8) from any initial configuration in $\mathcal{F} \setminus \mathcal{T}$ to "touch" the boundary $\partial\mathcal{T}$ of the target $\mathcal{T}$ in minimal time.
We remind that the occurrence of a singular control has been excluded and we expect to find a constant or a piecewise constant optimal control.
Let us distinguish several cases as done in the previous section.

5.1 | Case I : $\mathbf{z}^* \in \mathcal{F}_0$

In this subsection, we will give a characterization of the optimal control for any initial state $\mathbf{z}_0$ in the controllability set. More precisely, we will prove that the optimal control is given by a constant function or by a bang-bang one. In this last case, we will show that there exists a unique switching time where the control passes from 0 to 1.
Finally, we will observe that the switching curve, where the optimal control passes from 0 to 1, is part of $\Gamma_1^{\mathbf{z}^*} \cup \Gamma_1^{\mathbf{z}^\#}$.

Proposition 5. Assume $\mathbf{z}^* \in \mathcal{F}_0$. The optimal control law that drives any $\mathbf{z}_0 \in \mathcal{S}_1$ in $\mathcal{T}$ is the constant function $u = 0$ or the bang-bang one that switches from 0 to 1 in a state of $\Gamma_1^{\mathbf{z}^*}$.

Proof. □

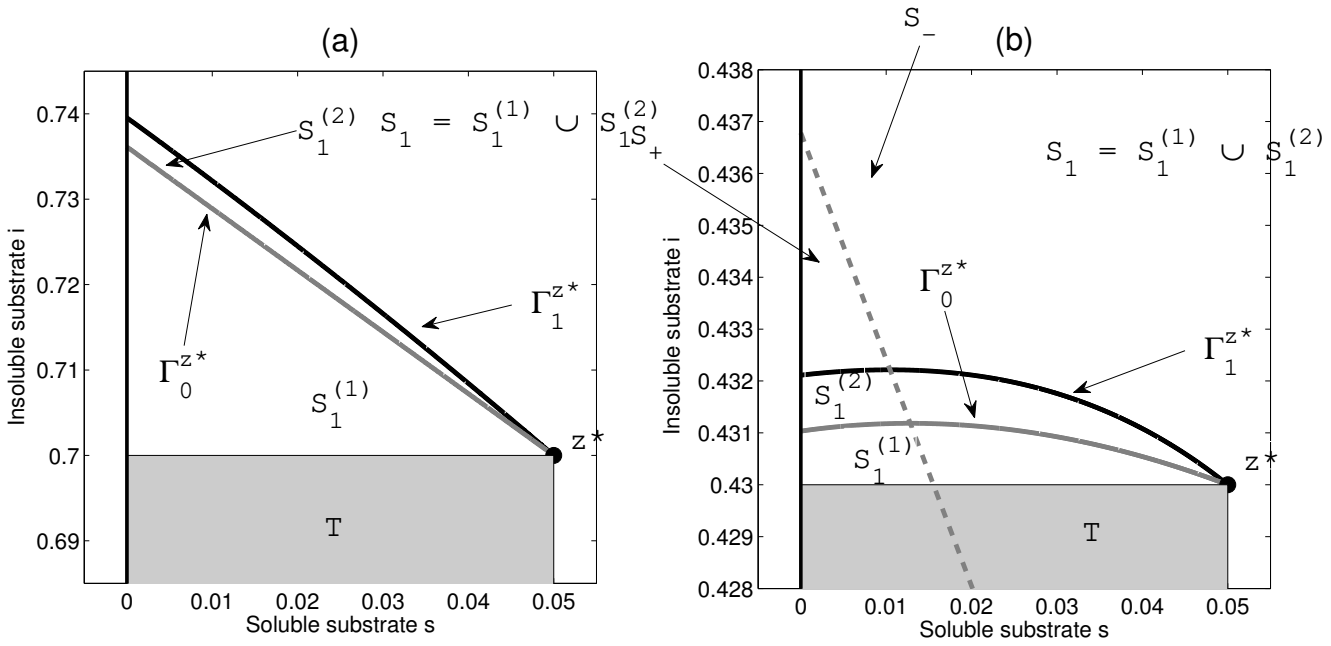

FIGURE 6 Zoom of the controllability set $\mathcal{S}_1$ when $\mathbf{z}^* \in \mathcal{F}_0$ in the case of Monod response functions (6). The nondimensional parameters values are given in (13). Two different scenarios have to be taken into account: (a) $\mathcal{S}_1 \cap \mathcal{S}_+ = \emptyset$ and (b) $\mathcal{S}_1 \cap \mathcal{S}_+ \neq \emptyset$, where $\mathcal{S}_+$ is given in (28).

We distinguish two cases.
Case (i). Let us suppose that $\mathcal{S}_1 \cap \mathcal{S}_+ = \emptyset$ (see Figures 6(a) and 7), where $\mathcal{S}_+$ has been introduced in (28).

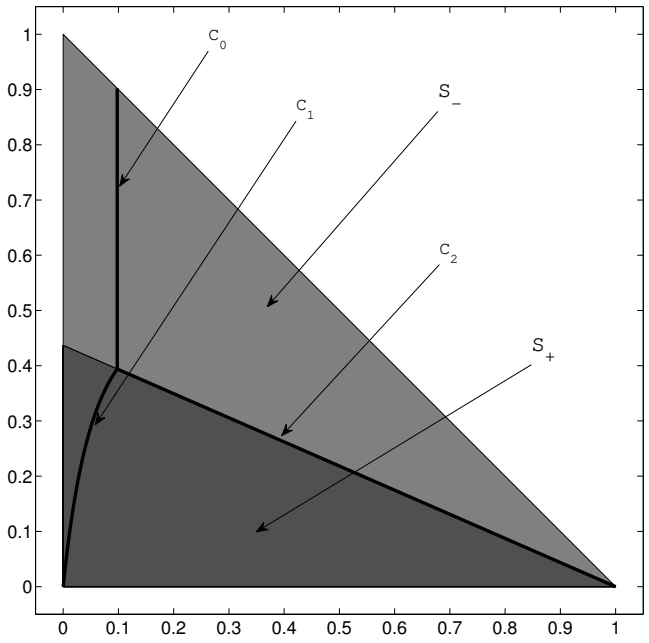

FIGURE 7 Partition (34) and subsets $\mathcal{S}_{\pm}$ (28)in the case of Monod response functions (6). The nondimensional parameters values are given in (13). We observe here that $\mathcal{F}_0 \cap \mathcal{S}_- \neq \emptyset$, $\mathcal{F}_0 \cap \mathcal{S}_+ \neq \emptyset$, $\mathcal{F}_1 \subset \mathcal{S}_+$ and $\mathcal{F}_2 \subset \mathcal{S}_-$.

First, we can observe that the optimal control must be $u = 1$ for any $\mathbf{z}_0 \in \Gamma_1^{\mathbf{z}^*}$ to prevent that the corresponding solution exits from the controllability set $\mathcal{S}_1$.

Let us consider a partition of $\mathcal{S}_1 = \mathcal{S}_1^{(1)} \cup \mathcal{S}_1^{(2)}$ where $\mathcal{S}_1^{(1)}$ is bounded by $\Gamma_0^{\mathbf{z}^*}$, $\mathcal{J}_2$ and the upper horizontal edge of $\mathcal{T}$ and $\mathcal{S}_1^{(2)} = \mathcal{S}_1 \setminus \mathcal{S}_1^{(1)}$ (see Figure 6(a)).

Let $\mathbf{z}_0$ be a state in $\mathcal{S}_1^{(1)}$. The solution starting from it reaches the target $\mathcal{T}$ on the upper horizontal edge in a state $(s(t_f), i^*)$ where $s(t_f) < s^*$. From the generalized transversality condition[5], it follows that $\lambda_s(t_f) = 0$, $\lambda_i(t_f) < 0$ (from (30)) and $\dot{\lambda}_s < 0$ (from (15)). Therefore $\lambda_s > 0$ in a left neighborhood of t_f and $\phi < 0$ from (19); hence the optimal trajectory reaches $\mathcal{T}$ with control $u = 0$. Since $\mathcal{S}_1 \subset \mathcal{S}_-$ (where $\mathcal{S}_-$ is defined in (28)), there cannot exist a switching time $t_1 < t_f$ where the control passes from 1 to 0. Therefore the constant $u = 0$ is optimal.

Now, let $\mathbf{z}_0$ be a state in $\mathcal{S}_1^{(2)}$. The target is reached with control $u = 1$ in the vertex $\mathbf{z}^*$. A control $u = 1$ is not compatible with the transversality condition when the final state is such that $s(t_f) < s^*$. In fact, the transversality condition on the upper horizontal edge of $\mathcal{T}$ gives $\lambda_s(t_f) < 0$, $\lambda_i(t_f) < 0$ and $\dot{\lambda}_s(t_f) < 0$ respectively from (30) and (15). This implies that $\lambda_s > 0$, $\phi < 0$ (from (19)) and $u = 0$ (from (18)) in a left neighborhood of t_f.

This means that the optimal trajectory leaves the initial state $\mathbf{z}_0$ with control $u = 0$ until it crosses $\Gamma_1^{\mathbf{z}^*}$; then the control switches from 0 to 1.

Case (ii). We suppose now that $\mathcal{S}_1 \cap \mathcal{S}_+ \neq \emptyset$ (see Figure 6(b) and 7).

The analysis is the same as above for states in $\mathcal{S}_1 \cap \mathcal{S}_-$. If $\mathbf{z}_0 \in \mathcal{S}_1 \cap \mathcal{S}_+$, according to Proposition 1, a switching from 1 to 0 can occur. Let $t_1 < t_f$ be a switching time. We can observe that the control is given by $u = 0$ in (t_1, t_f) and $\dot{\lambda}_s(t) - \dot{\lambda}_i(t) = c_h \left(\lambda_s(t) - \lambda_i(t)\right)$ for any $t \in (t_1, t_f)$. Moreover $\left(\lambda_s(t_1) - \lambda_i(t_1)\right)\left(\lambda_s(t_f) - \lambda_i(t_f)\right) < 0$ and $\left(\dot{\lambda}_s(t_1) - \dot{\lambda}_i(t_1)\right)\left(\dot{\lambda}_s(t_f) - \dot{\lambda}_i(t_f)\right) < 0$. It follows that there exists a time $t_2 \in (t_1, t_f)$ such that $\dot{\lambda}_s(t_2) - \dot{\lambda}_i(t_2) = 0 \neq \lambda_s(t_2) - \lambda_i(t_2)$ and thus a contradiction.

Proposition 6. *Case (i)*: $\Gamma_1^{\mathbf{z}^\#} \cap \mathcal{J}_0 \neq \emptyset$ (see panels (a) and (c) in Figure 3). The optimal control law that drives any $\mathbf{z}_0 \in \mathcal{S}_2$ in $\mathcal{T}$ is the constant function $u = 1$.

Case (ii): $\Gamma_1^{\mathbf{z}^\#} \cap \mathcal{J}_2 \neq \emptyset$ (see panels (b) and (d) in Figure 3).The optimal control driving any $\mathbf{z}_0 \in \mathcal{S}_2$ in $\mathcal{T}$ is the constant function $u = 1$.

Proof. Consider *Case (i)*. We observe that the optimal control must be $u = 1$ for any $\mathbf{z}_0 \in \Gamma_1^{\mathbf{z}^\#}$ to prevent that the corresponding solution exits from the controllability set $\mathcal{S}_2$.
For any state $\mathbf{z}_0$ in the interior of $\mathcal{S}_2$, the corresponding optimal solution cannot reach the target $\mathcal{T}$ with control $u = 0$, because the variable s would be increasing. Moreover, from Proposition 1, we can exclude a switching from 0 to 1, since $\mathcal{S}_2 \subset \mathcal{S}_+$ (see panels (a) and (c) in Figure 3 and Figure 7). Therefore, we can conclude that the optimal control is given by the constant function $u = 1$.
As concerns *Case (ii)*, if $\mathbf{z}_0 \in \mathcal{S}_2 \cap \mathcal{S}_+$ (see panels (b) and (d) in Figure 3 and Figure 7) the result is proved as in case (i).
In the case of $\mathbf{z}_0 \in \mathcal{S}_2 \cap \mathcal{S}_-$ the occurrence of a switching time is not excluded. Let $t_1 < t_f$ be a switching time where the control passes from 0 to 1. We observe that $u = 1$ in (t_1, t_f) and

$$\dot{\lambda}_s(t) - \dot{\lambda}_i(t) = c_h \left(\lambda_s(t) - \lambda_i(t)\right) - \lambda_s(t) g_1'(s(t))(1 - s(t) - i(t)) ;$$

therefore, $\dot{\lambda}_s - \dot{\lambda}_i$ must be positive when $\lambda_s - \lambda_i = 0$. It is easy to check that $\lambda_s(t_1) - \lambda_i(t_1) > 0 > \lambda_s(t_f) - \lambda_i(t_f)$ and, as consequence, there exist a time such that $\lambda_s - \lambda_i$ vanishes and passes from positive to negative values. Thus we have a contradiction. □

Proposition 7. Let $\Gamma_1^{\mathbf{z}^\#} \cap \mathcal{J}_2 \neq \emptyset$. The optimal control driving any $\mathbf{z}_0 \in \mathcal{F} \setminus \left(\mathcal{T} \cup \mathcal{S}_1 \cup \mathcal{S}_2\right)$ in $\mathcal{T}$ is of bang-bang type and passes from 0 to 1 in correspondence of $\Gamma_1^{\mathbf{z}^\#}$.

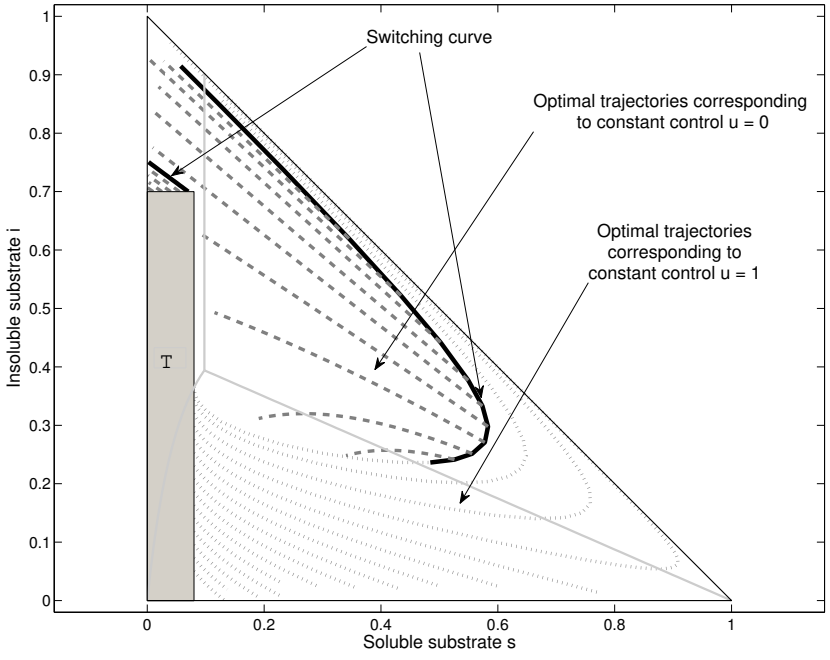

FIGURE 8 Optimal trajectories when $\mathbf{z}^* \in \mathcal{F}_0$ in the case of Monod response functions (6). The parameters values are given in (13). The controllability set is the whole invariant set $\mathcal{F}$. Continuous black lines denote the switching curve; dashed and dotted grey lines denote parts of the optimal trajectories where the control is $u = 0$ and $u = 1$, respectively.

Proof. A trajectory starting from $\mathbf{z}_0 \in \mathcal{F} \setminus \left(\mathcal{T} \cup \mathcal{S}_1 \cup \mathcal{S}_2\right)$ can reach the target passing through the subset $\mathcal{S}_2$. We observe that $\mathcal{S}_2$ is crossed by the optimal trajectory in presence of a constant control $u = 0$; from Proposition 6, the optimal control is given by $u = 1$ in $\mathcal{S}_2$. This means that there exists at least a switching time in correspondence of which the control passes from 0 to 1 and such switching occurs in a state of $\Gamma_1^{\mathbf{z}^*}$.
Moreover a switching from 1 to 0 in a state of $\left(\mathcal{F} \cap \mathcal{S}_-\right) \setminus \left(\mathcal{T} \cup \mathcal{S}_1 \cup \mathcal{S}_2\right)$ can be excluded as done in Proposition 5, by analyzing the quantity $\lambda_s - \lambda_i$. □

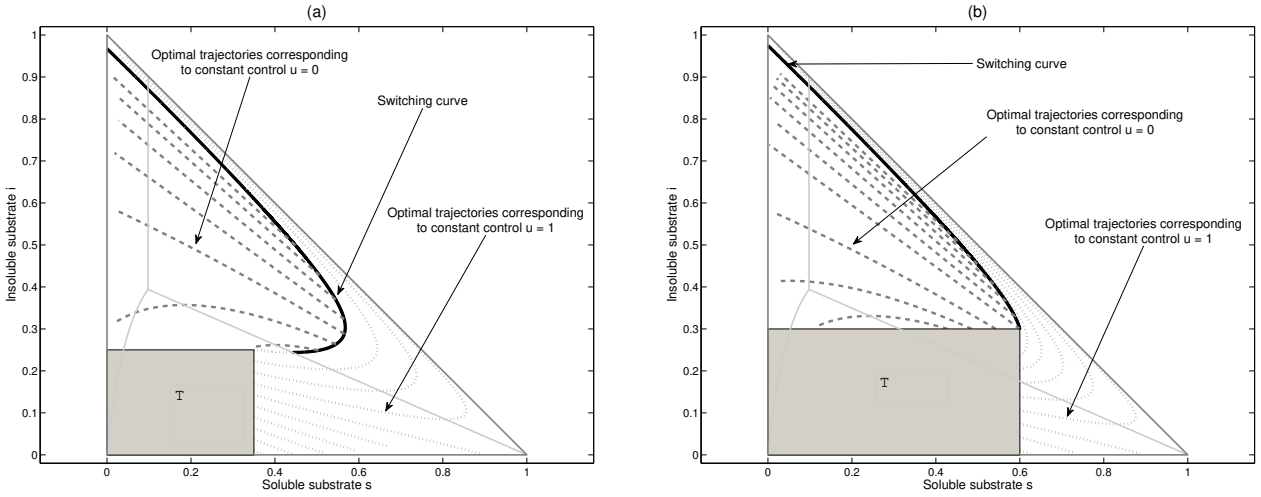

FIGURE 9 Optimal trajectories when $\mathbf{z}^* \in \mathcal{F}_1$ (a) and $\mathbf{z}^* \in \mathcal{F}_2$ (b) in the case of Monod response functions (6). The parameters values are given in (13). The controllability set is the whole invariant set $\mathcal{F}$. Continuous black lines denote the switching curve; dashed and dotted grey lines denote parts of the optimal trajectories where the control is $u = 0$ and $u = 1$, respectively.

We remark here that, if $\Gamma_1^{\mathbf{z}^\#} \cap \mathcal{J}_0 \neq \emptyset$, the target $\mathcal{T}$ is not reachable from a state in $\mathcal{F} \setminus \left(\mathcal{T} \cup \mathcal{S}_1 \cup \mathcal{S}_2\right)$, since the controllability set is given by $\mathcal{S}_1 \cup \mathcal{S}_2$ (see Proposition 2 and panel (c) in Figure 3).
Optimal trajectories are depicted in Figure 8 in the case of a Monod response function (6) when the controllability set coincides with the whole invariant set $\mathcal{F}$. The switching curve belongs to $\Gamma_1^{\mathbf{z}^*} \cup \Gamma_1^{\mathbf{z}^\#}$.

5.2 | Case II ($\mathbf{z}^* \in \mathcal{F}_1$) and Case III ($\mathbf{z}^* \in \mathcal{F}_2$)

In this subsection, we look for the optimal controls for any initial state $\mathbf{z}_0$ in the controllability set of the target $\mathcal{T}$, when its vertex $\mathbf{z}^*$ is in $\mathcal{F}_1$ or $\mathcal{F}_2$.

Proposition 8. *(i)* If $\mathbf{z}^* \in \mathcal{F}_1$, for any $\mathbf{z}_0 \in \mathcal{S}$ the optimal control is the constant function $u = 1$; the optimal control is of bang-bang type, if $\mathbf{z}_0 \in \mathcal{F} \setminus (\mathcal{T} \cup \mathcal{S})$, and it switches from 0 to 1 in a state of $\Gamma_1^{\mathbf{z}^*}$, when the controllability set is $\mathcal{F}$.
(ii) If $\mathbf{z}^* \in \mathcal{F}_2$ the optimal control law that drives any $\mathbf{z}_0 \in \mathcal{S}_1^{(1)}$ in $\mathcal{T}$ is the constant function $u = 0$ while the one that drives $\mathbf{z}_0 \in \mathcal{S}_2$ in $\mathcal{T}$ is $u = 1$. The optimal control is of bang-bang type, if $\mathbf{z}_0 \in \mathcal{S}_1^{(2)}$ and switches from 0 to 1 in a state of $\Gamma_1^{\mathbf{z}^*}$.

Proof. (i) The result can be proved as in Propositions 6, 8; the role of $\Gamma_1^{\mathbf{z}^\#}$ in case I is now played by $\Gamma_1^{\mathbf{z}^*}$. *(ii)* The result is proved as in Propositions 5, 6. □

The optimal trajectories and the the switching curves are depicted in Figure 9(a), when $\mathbf{z}^* \in \mathcal{F}_1$ and the controllability set in the whole invariant set $\mathcal{F}$, and in Figure 9(b), when $\mathbf{z}^* \in \mathcal{F}_2$.

6 | CONCLUSIONS

The aerobic degradation plays a crucial role in the composting plant and its mathematical modeling in the organic waste management is a very useful tool, especially in determining the optimal strategies to be adopted to improve plant performances.
In this context we have proposed a mathematical model for aerobic degradation of a two component substrate in a composting biocell and formulated a suitable time optimal control problem, whose main purpose is the reduction of the soluble and insoluble substrates below a given threshold. Such reduction is realized by controlling the effects of cell oxygen concentration on the degradation phenomenon.
For any target we have determined the controllability set, i.e. the set of configurations that can be driven to the target in finite time

by an admissible control, and observed that such set does not always coincide with the invariant set of admissible configurations. The results have been obtained for the non-dimensional variables and parameters; obviously, it is possible to deduce some indications in terms of the biological quantities. As example, we consider a test case, where the numerical values of initial soluble substrate, insoluble substrate and biomass are inspired by [13]. More precisely, the initial configuration proposed in [13] is given by

$$S(0) = 660\,Kg/m^3\,,\ I(0) = 1080\,Kg/m^3\,,\ X(0) = 0.4\,Kg/m^3\,, \tag{35}$$

corresponding to the pair $(s(0), i(0)) = (0.3792, 0.6206)$ (consequently, from (2) $x(0) = 0.0002$)[1].

For such configuration and parameters given in (13), a target with corner $(s^*, i^*) = (0.065, 0.7)$ (corresponding to $(S^*, I^*) = (113.13\,Kg/m^3, 1218.28\,Kg/m^3)$) cannot be reached in finite time (see Figure 3(a)). On the contrary, if the target corner is given by $s^* = 0.075$ and $i^* = 0.7$ (corresponding to $(S^*, I^*) = (130.53\,Kg/m^3, 1218.28\,Kg/m^3)$), then the target can be reached in finite time by assuming a constant control $u = 1$, since $(s(0), i(0)) \in \mathcal{S}_2$ (see Figure 3(b)).

The analysis shows that, if it is possible to regulate the initial amount of each component, it is required to carefully compose the initial mix of substrate and bacterial population in order to well balance the effects of digestion, hydrolysis and biomass decay processes along the entire evolution. In particular, for the target individuated by $(s^*, i^*) = (0.065, 0.7)$, only initial configurations in $\mathcal{S}_1$ (for example $(s(0), i(0)) = (0.03, 0.72)$, corresponding to $(S(0), I(0)) = (52.21\,Kg/m^3, 1253.09\,Kg/m^3)$) and in $\mathcal{S}_2$ (for example $(s(0), i(0)) = (0.4, 0.1)$, corresponding to $(S(0), I(0)) = (696.16\,Kg/m^3, 174.04\,Kg/m^3)$) can be steered to the target in finite time.

The optimal control and the corresponding trajectories have been determined for any initial state in the controllability set. We have proved that the optimal control time profiles can be constant (bang controls) or piecewise constant (bang-bang), assuming just minimal (control $u = 0$ corresponding to the absence of degradation) or maximal value (control $u = 1$ corresponding to the best performing admissible degradation).

In case of bang-bang control, the optimal control has a unique switching time at which it switches from 0 to 1 and the corresponding switching curve has been determined (see Propositions 5, 7, 8). This means that it is optimal to not control the system for an initial period and let the system to be driven by hydrolysis and biomass decay only. In the case of constant control, two different scenarios are admissible according to the initial state and target set. In the first scenario (Proposition 5), we have observed that, if the initial substrate concentration s_0 is already below the given the given threshold s^* and the insoluble component i_0 is sufficiently close to its corresponding threshold i^*, then it is optimal to not control the system ($u = 0$). In the second scenario (Proposition 6), when the initial insoluble component i_0 is already below the corresponding threshold i^* and the soluble substrate concentration s_0 is sufficiently close to the given threshold s^*, then it is necessary to control the system with maximum control ($u = 1$) so that the digestion process plays the key role in the evolution of the biological system.

ACKNOWLEDGEMENTS

This work was performed in the framework of INdAM-INGV joint project *Strategic Initiatives for the Environment and Security* (SIES) supported by MIUR (Progetto Premiale FOE2014). We thank the anonymous reviewers for their careful reading of our manuscript and their insightful comments and suggestions.

References

1. Bayen T., Cots O., Gajardo P. Analysis of an optimal control problem related to anaerobic digestion process. *J. Optim. Theory Appl.* 2018;178(2):627-659.

2. Bayen, T., Gajardo, P. On the steady state optimization of the biogas production in a two-stage anaerobic digestion model. *J. Math. Biol.* 2019;78(4):1067-1087.

3. Bayen T., Harmand J., Sebbah M. Time-optimal control of concentration changes in the chemostat with one single species. *Appl. Math. Model.* 2017;50:257-278.

[1] In [13] the values have been set as 2200, 3600,2 mol/m^3 for soluble substrate, insoluble substrate and biomass, respectively. The concentrations are then measured with given nominal molecular weights, i.e. 300 g/mol, 300 g/mol, 200 g/mol, respectively.

4. Borisov M., Dimitrova N., Beschkov V. Stability analysis of a bioreactor model for biodegradation of xenobiotics. *Comput. Math. Appl.* 2012;64(3):361-373.

5. Boscain U., Piccoli B. *Optimal syntheses for control systems on 2-D manifolds*. Springer Science & Business Media; 2004.

6. Bozkurt S., Moreno L., Neretnieks I. Long-term processes in waste deposits. *Sci. Total Environ.* 2000;250(1-3):101-121.

7. Cooperband L. *The art and science of composting*. Center for Integrated agricultural systems; 2002. https://www.cias.wisc.edu/wp-content/uploads/2008/07/artofcompost.pdf (accessed on February 2019)

8. Fleming W., Rishel R.W. *Deterministic and stochastic optimal control*. Springer Science & Business Media; 2012.

9. Hamelers H. V. M. *A mathematical model for composting kinetics*; 2001. http://library.wur.nl/WebQuery/wurpubs/fulltext/193815 (accessed on March 2018).

10. Haug R. T. *The Practical Handbook of Compost Engineering*. Boca Raton, FL: Lewis Publishers; 1993.

11. Husain A. Mathematical models of the kinetics of anaerobic digestion - a selected review. *Biomass Bioenerg.* 1998;14(5-6):561-571.

12. Liberzon D. *Calculus of variations and optimal control theory: a concise introduction*. Princeton University Press; 2011.

13. Lin Y. P., Huang G. H., Lu H. W., He L. Modeling of substrate degradation and oxygen consumption in waste composting processes. *Waste Manage.* 2008;28(8):1375-1385.

14. Lokshina L. Ya, Vavilin V. A. Kinetic analysis of the key stages of low temperature methanogenesis. *Ecol. Model.* 1999;117(2-3):285-303.

15. Martalò G., Bianchi C., Buonomo B., Chiappini M., Vespri V. Mathematical modeling of oxygen control in biocell composting plants. 2018. (submitted)

16. Martalò G., Bianchi C., Buonomo B., Chiappini M., Vespri V. On the role of inhibition processes in modeling control strategies for composting plants. 2018. (to appear in SEMA SIMAI Springer Series).

17. Monod J. *Recherches sur la croissance des cultures bacteriennes*; 1942.

18. Pacey J., Augenstein D., Morck R., Reinhart D., Yazdani R. *The bioreactor landfill-an innovation in solid waste management*. In *MSW Management*; 1999. http://citeseerx.ist.psu.edu/viewdoc/download?doi=10.1.1.460.2984&rep=rep1&type=pdf (accessed on April 2019).

19. Perko L. *Differential equations and dynamical systems*. Springer Science & Business Media; 2013.

20. Rada E. C., Ragazzi M., Villotti S., Torretta V. Sewage sludge drying by energy recovery from OFMSW composting: Preliminary feasibility evaluation. *Waste Manage.* 2014;34(5):859-866.

21. Pontryagin L. S. *Mathematical theory of optimal processes*. CRC Press; 1987.

22. Polprasert C. *Organic waste recycling*. John Wiley and Sons Ltd.; 1989.

23. Rapaport A., Bayen T., Sebbah M., Donoso-Bravo A., Torrico A. Dynamical modeling and optimal control of landfills. *Math. Models Meth. Appl. Sci.* 2016;26(5):901-929.

24. Seng B., Kaneko H. *Simulation of windrow composting for organic solid wastes*. Bangkok. International Conference on Chemical, Biological and Environment Sciences (ICCEBS'2011); 2011.

25. Seng B., Kristanti R. A., Hadibarata T., Hirayama K., Katayama-Hirayama K., Kaneko H. Mathematical model of organic substrate degradation in solid waste windrow composting. *Bioprocess. Biosyst. Eng.* 2016;39(1):81-94.

26. Servizi Pubblici Locali. http://www.spl.invitalia.it/site/spl/home/osservatorio-spl/monitor-ato/gestione-rifiuti-urbani.html. (accessed on March 2018 - in italian)

27. Schaettler H., Ledzewicz U. *Geometric optimal control: theory, methods and examples*. Springer Science & Business Media; 2012.

28. Vavilin V. A., Rytov S. V., Lokshina L. Y., Pavlostathis S. G., Barlaz M. A. Distributed model of solid waste anaerobic digestion: effects of leachate recirculation and pH adjustment. *Biotechnol Bioeng.* 2003;81(1):66-73.